



AEROACOUSTIC MEASUREMENT OF AUTOMOTIVE HVAC IN-DUCT ELEMENTS

Saâd BENNOUNA^{1,2}, Boureima OUEDRAOGO¹,
Solène MOREAU¹, Jean-Michel VILLE¹, Olivier CHERIAUX²

¹ *Sorbonne Universités, Université de Technologie de Compiègne,
Laboratoire Roberval - UMR CNRS 7337, CS 60319, 60203 Compiègne
cedex, France*

² *Valeo Thermal Systems, 8 rue Louis Lormand, 78320 La Verrière, France*

SUMMARY

Passengers' thermal comfort is mainly provided by the Heating Ventilation and Air Conditioning (HVAC) module. Air provided by HVAC is blown via a blower, passing through HVAC components and then distributed to different areas. To blow the air inside the cabin, the blower must overcome the pressure loss generated by the elements inside the HVAC module. Due to this fact, noise is naturally created. Valeo, as an HVAC supplier, has identified the annoying sources. Several studies between Valeo and universities have been done and are ongoing to simulate those noise cases. Valeo is aiming, through CEVAS project, to develop a prediction tool which will provide spectrum and sound quality data. The final output of the project is a numerical muck up which will be available for the designer as a guideline. The tool will be based, in particular, on aeroacoustic measurements based on 2N ports source and Particle Image Velocimetry methods to provide characteristics of passive and active HVAC components.

INTRODUCTION

Generated noise inside car cabin depends on many sources such as thermal engine and embedded equipments like the HVAC module. Currently, HVAC noise is becoming a crucial issue since engine noise is reduced for silent thermal vehicles and further for hybrid and electric vehicles. The issue is then critical for car makers who are willing to improve the acoustic comfort inside car cabin.

In this context, automotive suppliers are working to predict and reduce HVAC noise. For instance, Valeo has developed simulation tools to predict HVAC overall noise level and spectrum. These methods are based on HVAC aeraulic performances and allow Valeo to evaluate HVAC design concepts during development stages. Each concept gives indications for potential improvements and then allows Valeo to produce an optimized HVAC module.

Thus, through CEVAS project, Valeo is aiming to improve its prediction methods by developing a tool [1] which will provide HVAC noise spectrum and sound quality data. This tool will require

acoustic and aeraulic experimental measurements to achieve the aeroacoustic characteristics of passive (flaps, thermal exchangers, grids) and (blower) elements.

A test bench based on Valeo’s specifications has been developed and built under CESAM project [2] by the acoustic laboratory of the University of Technology of Compiègne (UTC). The bench describes an HVAC component as a 2N-port source represented by its passive and active acoustic properties. To measure aeraulic data, the bench is now equipped with Particle Image Velocimetry (PIV) method.

In this paper, HVAC and its components are presented. Thereafter the experimental test bench is described including experimental setup and data processing.

HEATING VENTILATION AND AIR CONDITIONNING SYSTEM

System description

To ensure its thermal functions, an HVAC is composed of many components: flaps, thermal exchangers, blower and many ducts to distribute airflow towards car cabin areas. Because of packaging constraints under dashboard and according to car maker specifications, many different HVAC system architectures are available. HVAC components are gathered in four blocks as presented in Figure 1 : Air Inlet block, Blower, Thermal block and Distribution block.

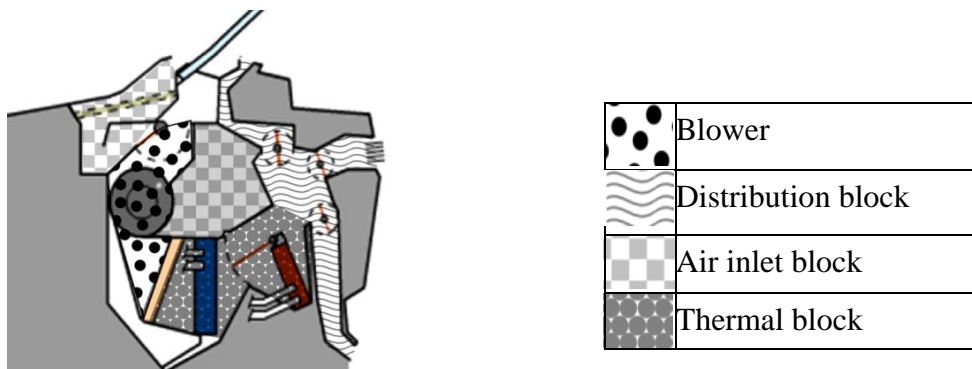


Figure 1: Structure of an HVAC module.

System operating

HVAC systems are based on air circulation. Firstly, air is collected whether at windshield’s base outside car or inside car cabin using recirculation inlet. Inside the air inlet block, air is blown by the blower and then filtered. Then, air is heated or cooled by the thermal exchangers and mixed in the thermal block. Finally, in the distribution block, air is distributed into car cabin areas. The air circulation path is presented in Figure 2.

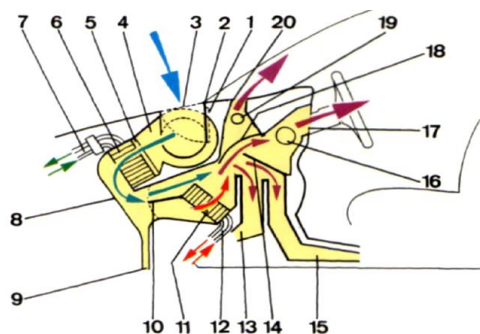


Figure 2: HVAC module operating. 1.Recirculation air inlet – 2.Air inlet flap – 3.Outside fresh air – 4.Blower – 5.Air filter – 6.Evaporator – 7.Refrigerant A/C Loop – 8.HVAC Structure – 9.Condensate outlet – 10.Mixing air flap – 11.Heater – 12.Heater water loop – 13, 15, 16, 17, 19, 20.Air outlet – 14.Air distribution Flap – 18.Defogging/demisting flap.

Noise definition

An HVAC is a complex system composed of various components. Due to its design many noises of several origins occur within it. Figure 3 shows HVAC's main Noise Vibration and Harshness (NVH) issues.

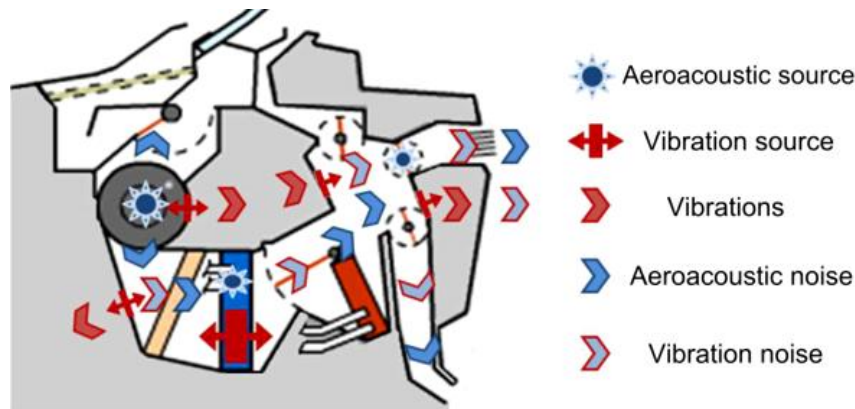


Figure 3: HVAC's noise and vibration sources.

The following HVAC's NVH issues are very none by the suppliers. Different approaches were done to identify root causes and provide guidelines to solve them [3].

- Engine stop noise: Vehicles equipped with start and stop system or hybrid vehicles are subject to hidden noises. When thermal engines are switched off, HVAC noises emerge in car cabin.
- Air flow noise: HVAC produces air flow up to 600 Kg/h. Due to air flow speed, HVAC pressure and blower wheel velocity, broad band noise is created inside car cabin. Also, interaction between air flow and HVAC components, such as flaps, creates turbulences which are responsible of air flow noises inside car cabin.
- Harmonic noise: Currently, blower motors used by Valeo and its competitors such as brush type motors as represented in Figure 4. The corresponding rotor includes 12 slots. During operation slot/brush contact creates harmonic 12 vibrations which are transmitted to motor cover and are emerged as noise.

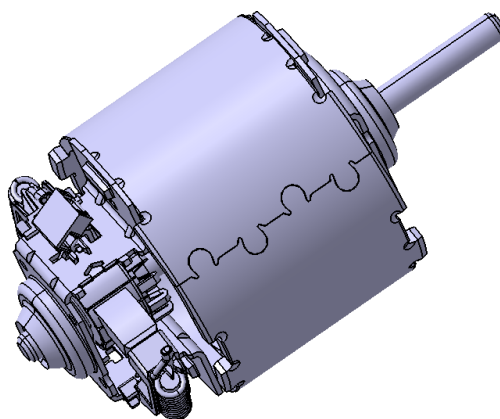


Figure 4: HVAC motor.

- Ticking noise: Motor commutator surface is not perfectly smooth and contains microscopic defaults. At low blower speed and low air flow, vibration is transmitted to all motor components including motor cover which transmits noise.

EXPERIMENTAL TEST BENCH

Bench description

Under CESAM and CEVAS projects, UTC has developed an experimental test bench to measure acoustic and aeraulic properties of HVAC components. The test bench is presented in Figure 5.

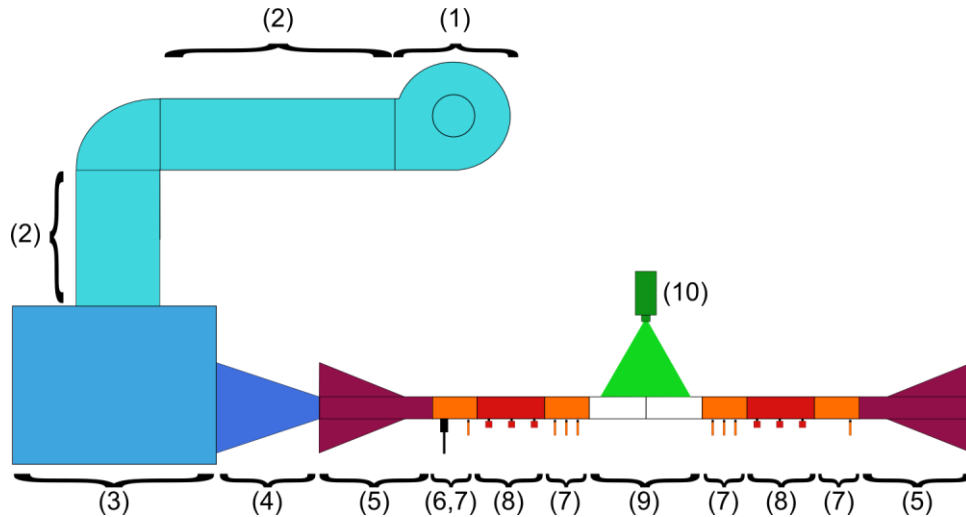


Figure 5: Test bench's description.

The first part of the bench is designed to generate air flow. It is composed of a variable speed centrifugal fan (1), two straight mufflers (2), a flow tranquilizing box (3) and a flowmeter (4). This device, represented Figure 6, allows precise measurement of flowrate inside the duct (accuracy of 2.5% kg/h till 800 kg/h).



Figure 6: Test bench's flowmeter.

The second part of the bench, consists of a 200x100mm cross-section rectangular duct. The duct is divided in parts ensuring implementation of acoustic and aeraulic equipments to perform the measurements: two anechoic terminations (5), two acoustic source ducts (8), four acoustic measurement ducts (7) and a test duct (9) in which HVAC components are placed. The test duct is made in transparent material to ensure optical access for PIV measurements (10).

2N-ports model

2N-ports model allows an intrinsic acoustic linear description of an element inside a duct based on N propagative modes. Using this model, an element is described by its acoustic passive and active properties. The acoustic passive property consists of transmission and reflexion coefficients, acquired by measuring the multimodal scattering matrix. The acoustic active property consists of acoustic pressures generated by interaction between airflow and component, acquired by measuring the source vector. 2N-ports model is defined by

$$\begin{aligned} \{P^{out}\}_{2N} &= [S]_{2N \times 2N} \times \{P^{in}\}_{2N} + \{P^S\}_{2N} \\ \begin{Bmatrix} P_{mn}^{I-} \\ P_{mn}^{II+} \end{Bmatrix}_{2N} &= [S]_{2N \times 2N} \times \begin{Bmatrix} P_{mn}^{I+} \\ P_{mn}^{II-} \end{Bmatrix}_{2N} + \begin{Bmatrix} P_{mn}^{S+} \\ P_{mn}^{S-} \end{Bmatrix}_{2N} \end{aligned} \quad [1]$$

where $\{P^{out}\}_{2N}$ is the outgoing pressures vector, $\{P^{in}\}_{2N}$ the incoming pressures vector, $\{P^S\}_{2N}$ the source vector and $[S]_{2N \times 2N}$ the multimodal scattering matrix in presence of air flow. P_{mn}^{I+} , P_{mn}^{I-} , P_{mn}^{II+} and P_{mn}^{II-} are respectively the incident, reflected, transmitted and retrograde pressure vectors for (m, n) mode as presented in Figure 7. P_{mn}^{S-} and P_{mn}^{S+} are source vector components.

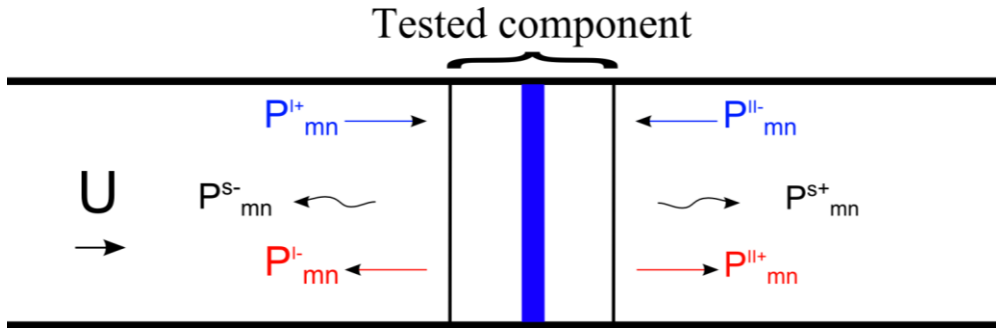


Figure 7: Representation of acoustic pressures inside duct.

Measurements method of acoustic active and passive properties requires two steps:

- Using 2N-sources method [4], measurement of scattering matrix $[S]_{2N \times 2N}$ and anechoic termination reflexion matrices $[R^{ter}]_{2N \times 2N}$
- Measurement of source vector $\{P^S\}_{2N}$ using components of scattering matrix $[S]_{2N \times 2N}$ and those of anechoic termination reflexion matrices $[R^{ter}]_{2N \times 2N}$.

Acoustic measurements instrumentation

2N-ports model requires acoustic source parts for scattering matrix measurements and microphone parts for scattering matrix and source vector measurements. The parts are placed on either side of measured component.

Acoustic source parts

Acoustic pressure field inside the duct is created by a speaker. The speaker is operated using a generator and a power amplifier. Excitation signal is a pseudo-random signal between 100Hz and 3700Hz. Pseudo-random signal consists of random phase and fixed amplitude. In order to offset airflow noise during acoustic measurements, excitation signal amplitude is increased in low frequencies. The awaited acoustic properties require 2N independent configurations of acoustic pressure field. The speaker is placed in N excitation positions of source part on either side of measured component as shown in Figure 8.

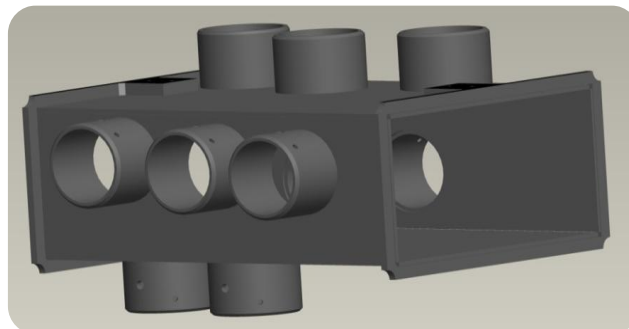


Figure 8: Acoustic excitation duct.

Acoustic measurements parts

Acoustic measurements are made using Brüel & Kjaer 4947 and GRAS 40AD microphones. The arrangement and the number of microphones are chosen to enable modal decomposition and wave separation steps leading to modal pressure vectors. In compliance with Shannon's criterion, four microphones per wavelength are used in order to extract the acoustic mode. Thus, eight microphones are fixed on the two horizontal walls and four microphones on the vertical one. The distance between two microphones is chosen to avoid acoustic pressure nodes. To improve wave separation, acoustic measurements are made using three microphone sections on either side of measured component. The distance between two sections is of 35 mm. The acoustic measurement part is illustrated in Figure 9.

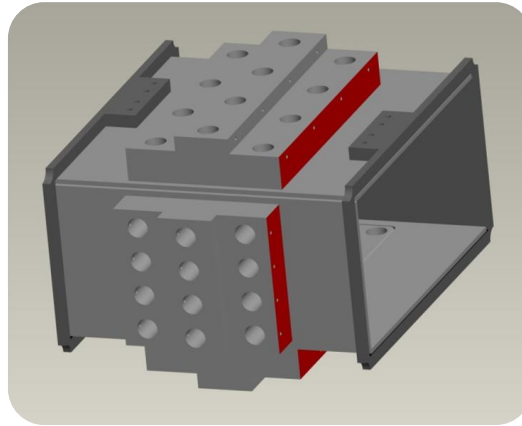


Figure 9: Acoustic measurement part.

Acoustic measurement procedure

Scattering matrix $[S]_{2N \times 2N}$

The required $2N$ configurations are obtained by moving the speaker on $2N$ positions of excitation ducts. Modal pressure vectors are measured using six microphone sections as presented in Figure 10.

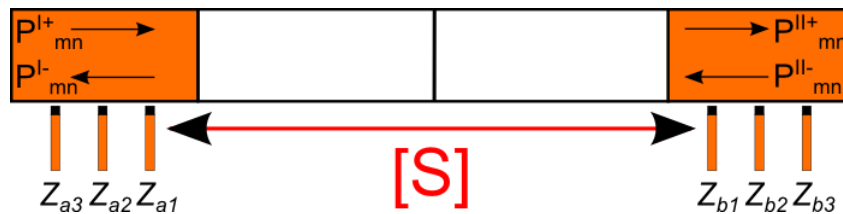


Figure 10: Scattering matrix measurement's configuration.

The measured data allows modal decomposition of acoustic pressure field on each microphone section. Wave separation provides incident and reflected modal pressure vectors for each microphone section. The incoming $[P^{in}]_{2N \times 2N}$ and outgoing $[P^{out}]_{2N \times 2N}$ pressure matrices are created. The scattering matrix is determined by solving

$$[S]_{2N \times 2N} = [P^{out}]_{2N \times 2N} \times [[P^{in}]_{2N \times 2N}]^{-1}. \quad [2]$$

The measurement procedure of multimodal scattering matrix is presented in Figure 11. Reflexion matrices of anechoic terminations are measured simultaneously with scattering matrix.

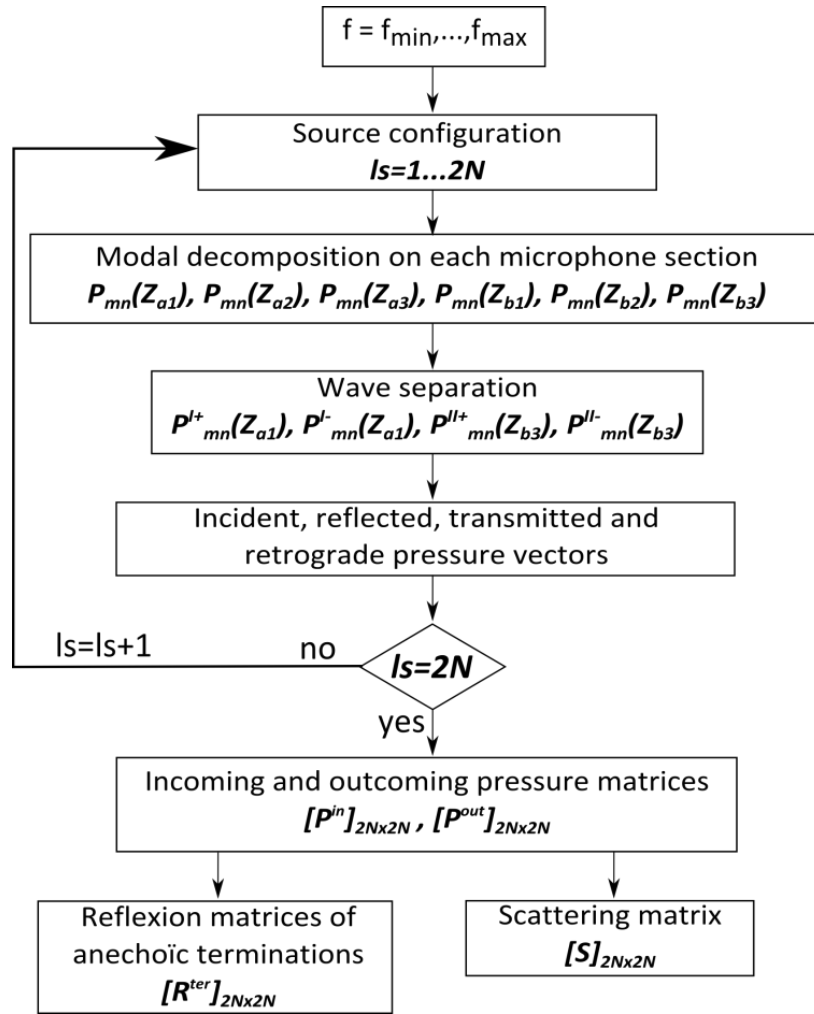


Figure 11: Scattering matrix measurement's procedure.

Source vector $\{P^S\}_{2N}$

Source vector is measured without using acoustic sources. Microphones are moved far from component to reduce turbulences effects on measurements. The measure requires four microphone sections as shown in Figure 12.

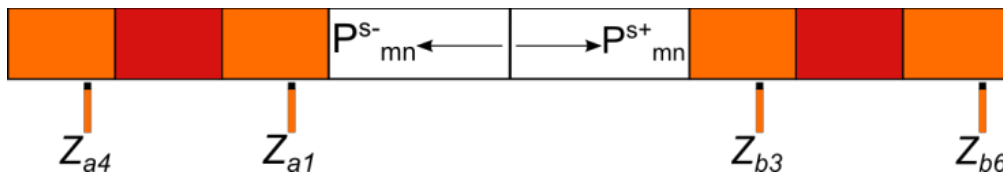


Figure 12: Source vector measurement's configuration.

Cross-spectrum are measured between four microphone sections to define the cross-microphone matrix

$$[G]_{2N_{mic} \times 2N_{mic}} = \begin{bmatrix} [[G_{a1a4}]] & [[G_{a1b4}]] \\ [[G_{b3a4}]] & [[G_{b3b4}]] \end{bmatrix}_{2N_{mic} \times 2N_{mic}} \quad (3)$$

Cross-spectrum matrix describes measured component as noise source

$$[G^S]_{2N \times 2N} = \begin{Bmatrix} P_{mn}^{S-}(Z_{a1}) \\ P_{mn}^{S+}(Z_{b3}) \end{Bmatrix}_{2N} \cdot \begin{Bmatrix} P_{mn}^{S-}(Z_{a1}) \\ P_{mn}^{S+}(Z_{b3}) \end{Bmatrix}_{2N}^c \quad (4)$$

where c denotes a complex conjugated quantity. The matrix is estimated using first step's data

$$[G^S]_{2N \times 2N} = [T^-]_{2N \times 2N} \cdot [C']_{2N \times 2N_{mic}} \cdot [G]_{2N_{mic} \times 2N_{mic}} \cdot [C']^c_{2N_{mic} \times 2N} \quad [5]$$

where

$$[C']_{2N \times 2N_{mic}} = [[I] - [S'] \cdot [R'^{ter}]]_{2N \times 2N} \cdot [\Pi']_{2N \times 2N_{mic}} \quad [6]$$

- $[I]$: identity matrix
- $[T^-]_{2N \times 2N}$: transfer matrix from measured quantities in Z_{a1}, Z_{b3} to quantities placed in Z_{a4}, Z_{b4} positions
- $[S']_{2N \times 2N}$: component's scattering matrix calculated in Z_{a4} and Z_{b4} sections
- $[R'^{ter}]_{2N \times 2N}$: anechoic terminations reflexion matrices calculated in Z_{a4} and Z_{b4} positions
- $[\Pi']_{2N \times 2N_{mic}}$: total pressures in Z_{a4} and Z_{b4} calculate from modal pressures.

Component's cross-spectrum matrix is defined by

$$[G^S]_{2N \times 2N} = \begin{bmatrix} [G^S_{a1a1}]_{N \times N} & [G^S_{a1b3}]_{N \times N} \\ [G^S_{b3a1}]_{N \times N} & [G^S_{b3b3}]_{N \times N} \end{bmatrix}_{2N \times 2N} \quad [7]$$

where

- $[G^S_{a1a1}]_{N \times N} = \{P^{S^-}(Z_{a1})\}_N \cdot \{P^{S^-}(Z_{a1})\}_N^c$: diagonal terms represent modal pressure levels created by airflow/component's interaction upstream component in Z_{a1} section
- $[G^S_{a1b3}]_{N \times N} = \{P^{S^-}(Z_{a1})\}_N \cdot \{P^{S^-}(Z_{b3})\}_N^c$: coherence between propagative modes in Z_{a1} and Z_{b3} sections with Z_{b3} reference section
- $[G^S_{b3a1}]_{N \times N} = \{P^{S^-}(Z_{b3})\}_N \cdot \{P^{S^-}(Z_{a1})\}_N^c$: coherence between propagative modes in Z_{a1} and Z_{b3} sections with Z_{a1} reference section. Off-diagonal terms can be used to deduce source's compactness [5]
- $[G^S_{b3b3}]_{N \times N} = \{P^{S^-}(Z_{b3})\}_N \cdot \{P^{S^-}(Z_{b3})\}_N^c$: diagonal terms represent modal pressure levels created by airflow/component's interaction downstream component in Z_{b3} section.

The measurement procedure of source vector is presented in Figure 13.

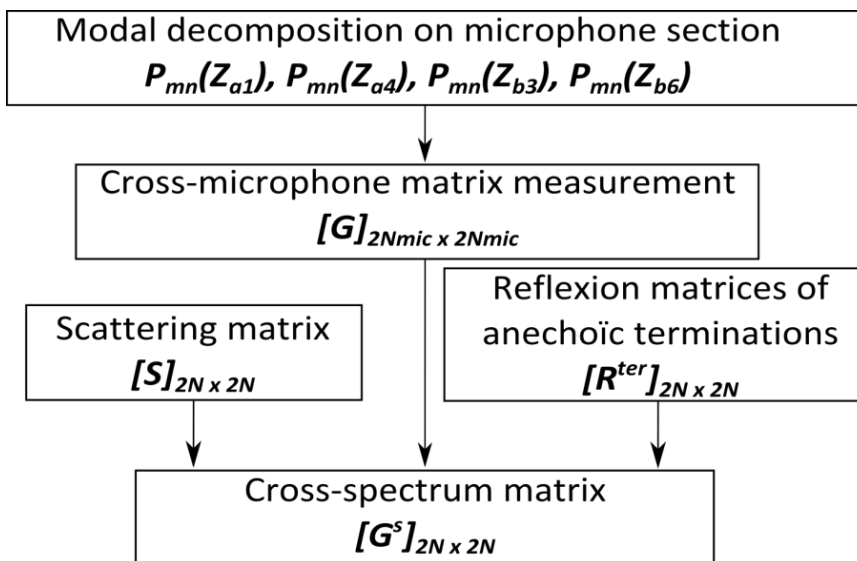


Figure 13: Source vector measurement's procedure.

Nelson and Morphey model

HVAC components can be described as in-duct aeroacoustic sources. The noise produced by the interaction between a low Mach number air flow and in-duct elements has been studied by Nelson and Morphey [6]. It has been shown that knowing components static pressure loss, the radiated acoustic power is proportional to coefficient K which depends on Strouhal number

$$St = fd/U \quad [8]$$

where f is the measurement frequency, d the component's characteristic dimension and U the airflow speed.

Nelson and Morphey model is based on the assumption that the RMS fluctuating drag force in a bandwidth acting on the component is proportional to the steady state drag force

$$(F_{drag})_{RMS,\Delta f} = K(St) \cdot \overline{F_{drag}} \quad [9]$$

where $\overline{F_{drag}}$ is the steady state drag force, $(F_{drag})_{RMS,\Delta f}$ the fluctuating drag force and Δf measurement bandwidth.

$K(St)$ coefficient is acquired using two semi-empirical equations depending on studied bandwidth.

$$f_c < f_0 \quad 20 \log_{10}(K(St)) + 120 = L_w(f_c) - 10 \log_{10} \left(\frac{\rho_0 A [\sigma^2 (1 - \sigma)]^2 C_D^2 U_c^4}{16 c_0} \right) \quad [10]$$

$$\begin{aligned} f_c > f_0 \quad 20 \log_{10}(K(St)) + 120 \\ = L_w(f_c) - 10 \log_{10} \left(\frac{\rho_0 \pi A^2 St^2 [\sigma^2 (1 - \sigma)]^2 C_D^2 U_c^6}{24 d^2 c_0^3} \right) \\ - 10 \log_{10} \left(1 + \left(\frac{3\pi c_0}{4w_c} \right) \left(\frac{a+b}{A} \right) \right) \end{aligned} \quad [11]$$

with $L_w(f_c)$ the radiated acoustic power (dB), $C_D = \frac{\Delta P}{0.5 \rho_0 U^2}$ the pressure loss coefficient, ρ_0 the air density ($\text{Kg} \cdot \text{m}^{-3}$), c_0 the sound speed (m/s), U the airflow speed upstream component (m/s), A the duct section (m^2), $\sigma = \frac{\sqrt{C_D - 1}}{C_D - 1}$ the open area ratio, f_0 the first transverse mode cut-on frequency (Hz) and ΔP the component static pressure loss (Pa). The characteristic dimension of the component is defined by $d = \sqrt{\frac{4A\sigma}{\pi}}$ [7].

Based on Nelson and Morphey theory, a single fixed HVAC component can be characterized leading to the acoustic power radiated by its interaction with airflow.

Acoustic attenuation

Mean airflow interacting with an in-duct element can dissipate or amplify the noise propagating [8]. Acoustic power attenuation provides quantified information about dissipation characteristics [4] and is defined by

$$Attenuation(dB) = 10 \log \left(\frac{W_{en}}{W_{so}} \right) \quad [12]$$

where W_{en} is the incoming acoustic power upstream the component and W_{so} the outgoing acoustic power downstream the component. Based on components scattering matrix, acoustic attenuation value establishes acoustic dissipation. If acoustic attenuation value is positive, component dissipates the acoustic energy. If acoustic attenuation value is negative, component amplifies the acoustic energy.

HVAC BLOWER

Experimental setup

In this section, the bench described previously is used on a HVAC blower. For the purpose of the study, the design of the blower is a realistic representation of HVAC geometry. To ensure optical access, the chosen geometry is designed in transparent material as presented in Figure 14.

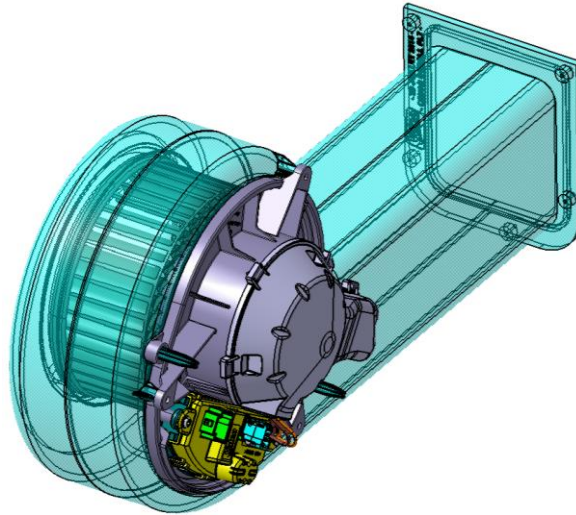


Figure 14: Blower design.

Blower's inlet consists of a circular cross section of 160 mm where the outlet consists of a rectangular section of 90x100 mm². To assemble the blower to the test bench, several fitting parts were used as presented in Figure 15.

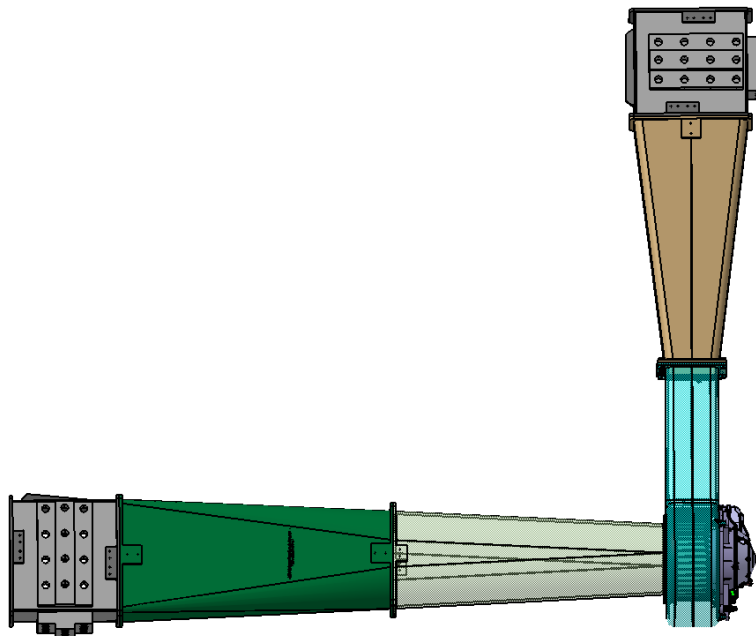


Figure 15: Blower assembly on test bench.

Blower's rotational speed is measured using a laser tachometer (Braun C118). An electric supply (Sorensen DLM 20-30), is used to supply the blower at its operating points.

Blower characterization also requires pressure loss measurements. Pressures are measured using two, flush mounted, pressure extraction points located upstream and downstream the blower.

Measurement configurations

Operating points of blower are defined according to Valeo's specifications and match pure HVAC ventilation modes (CVAF : Cold Ventilation Aeration Fresh, CVAR : Cold Ventilation Aeration Recycled, HFF : Hot Feet Fresh, HDF : Hot Defrost Fresh). Each ventilation mode is modeled by a pressure loss circuit as presented in Figure 16. Pressure loss circuits are generated by HVAC cavities and components (thermal exchangers, filters, flaps positions...).

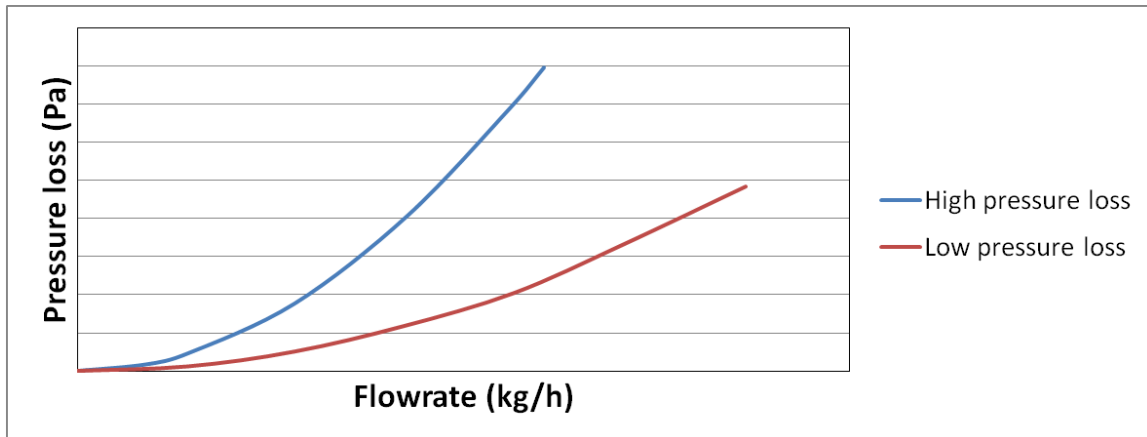


Figure 16: Blower's pressure loss circuits.

In this study, operating points corresponding to the four pure ventilation modes, are reached using flowrate and blower's rotation speed. To change the pressure loss of the bench, diaphragms are placed at the end of the downstream anechoic termination as presented Figure 17. Each diaphragm is designed to generate a pressure loss which matches an HVAC pure ventilation mode.

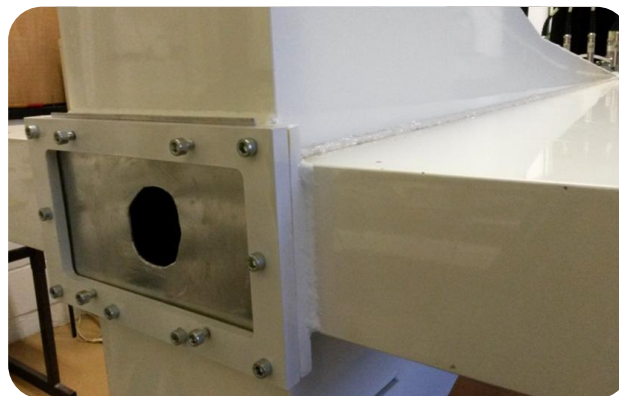


Figure 17: Pressure loss diaphragm.

CONCLUSION

This work presents an experimental facility to measure aeroacoustic properties of induct elements.

The measured elements properties are based on 2N-ports modeling which provide multimodal scattering matrix and source vector. From the measurements, Nelson and Morphe theory is applied to reach K coefficient and the acoustic attenuation is determined.

The studies were conducted on fixed elements (diaphragm, combination of diaphragms, flaps). Results indicated potential lines of improvements of the measuring procedures. Currently, these procedures are improved and will be applied to the HVAC blower.

ACKNOWLEDGEMENTS

This work is funded by the FEDER (Fond Européen de Développement Régional). These studies are conducted in the FUI project CEVAS involving industrial and academic partners : Valeo Thermal Systems, Cetim, ESI-Group, Genesis and the University of Technology of Compiègne.

BIBLIOGRAPHY

- [1] M. Legros, J.M. Ville, S. Moreau, Y. Goth, and X. Carniel, "Acoustic synthesis of an automotive HVAC," *FAN 2015 Congress*, 2015.
- [2] H Trabelsi, "Banc d'essai et procédure pour la caractérisation des éléments d'un HVAC par un système "2N-ports" avec écoulement : validation et application à des sources aéroacoustiques," 2011.
- [3] S. Naji and F. Ailloud, "Automotive HVAC unit noise prediction using blower dimensioning tool," in *5th automotive and railroad comfort symposium*, Le Mans, France, 2008.
- [4] A Sitel, "Méthodes de mesure des matrices acoustiques des discontinuités à un ou deux ports en présence des modes élevés," (2005).
- [5] M Abom and H Bodèn, "A note on the aeroacoustic source character of in-duct axial fans," *Journal of Sound and Vibration*, vol. 186, no. 4, pp. 589-598, 1995.
- [6] P. A. Nelson and C. L. Morfey, "Aerodynamic sound production in low speed flow ducts," *Journal of Sound and Vibration*, vol. 79, pp. 263-289, (1981).
- [7] Oscar Karekull, Gunilla Efraimsson, and Mats Abom, "Prediction model of flow duct constriction noise," *Applied Acoustics*, vol. 82, pp. 45-52, 2014.
- [8] P. Testud, Y. Aurégan, and A. Hirschberg, "Experimental validation of a whistling criterion for orifices in air pipe flow," in *SFA2006*, 2006.